PRELIMINARY RESULTS OF POST-SEISMIC DISPLACEMENT OF 2011 Mw 6.8 TARLAY EARTHQUAKE, MYANMAR USING TIME-SERIES INSAR TECHNIQUES

Pattama Phodee[a] and Anuphao Aobpaet[b]

[a] Ph.D. student, Department of Survey Engineering, Faculty of Engineering, Chulalongkorn University, Thailand;

E-mail: pattamaphodee@yahoo.com

[b] Geo-Informatics and Space Technology Development Agency (Public Organization),

165 Chalongkrung Road, Lad Krabang, Bangkok 10520 Thailand;

E-mail: Anuphao@eoc.gistda.or.th

KEY WORDS: Time-series InSAR, Post-seismic motion, Namma fault, Tarlay earthquake, Mae Chan fault

ABSTRACT: The co-seismic motion of Mw = 6.8 Tarlay earthquake of March 24 th, 2011 in Myanmar can be detected by InSAR over the upper-northern part of Thailand. Of especially interest is Mae Chan fault in Chiang Rai province which is located approximately 50 kilometers from the epicenter. A previous study using 2-pass DInSAR with ALOS-PALSAR images for both ascending and descending orbits, reveals rupture of more than 20 kilometers with approximately 1.2 meters offset in left-lateral sense and the re-distribution of stress may promote failure on certain segments of Mae Chan fault. This study aims to monitoring the characteristics of post-seismic deformation of Tarlay earthquake with also attention on stress change on Mae Chan fault. The study area is covered with dense vegetation and accessing to the study area is very difficult, so InSAR time-series technique is an attractive technique to measure surface deformation. Radarsat-2 data acquired from June 2011 to May 2012 have been processed by PSInSAR and Small Baseline techniques. The initial results with mean LOS deformations reveal the potential of Radarsat-2 data to estimate the surface deformation which occurred around Mae Chan fault. Further study will be performed on longer time-series Radarsat-2 data and modeling of post-seismic motion.

INTRODUCTION

There was Mw = 6.8 Tarlay earthquake in a segment of Nam Ma fault located in Myanmar on March 24 th, 2011. The hypocenter of this occurrence is approximately 10 kilometers below surface (McCaughey and Tapponnier, 2011). On May 16th, 2007 a Mw = 6.1 earthquake happened in Laos on a location that appears to be an eastern segment of Mae Chan fault as shown in figure 1. The close occurrence of these two events in both time and space seems to support stress transfer theory where an earthquake can trigger or suppress other earthquakes in nearby areas. And an interesting question is whether Mae Chan fault, particularly segments that pass through small town are closer to failure. Most of fault sets in the Golden Triangle area at the junction of Myanmar, Laos, and Thailand borders lineated north-eastern and south-western. Mae Chan fault which is situated in the northern part of Thailand was a left-lateral strike-slip fault with 101 kilometers long and was lineated from Fhang District to faults in Laos (Jitmahantakul, 2011). A previous study of Tarlay earthquake using 4 ALOS PALSAR imageries, both ascending and descending orbits, revealed a rupture of more than 20 kilometers [figure 2]. From the interferograms, there is approximately 1.2 meters left-lateral offset in line-of-sight direction across the fault (Trisirisatayawong et al., 2011). From the result, it could be inferred that the earthquake could also have an influence on Mae Chan fault.

The post-seismic investigation is very interesting according to a previous study mentioned above. Because, this is a procedure of energy accumulation which it could have a probability of earthquake in the future. However, Mae Chan fault area is covered by dense vegetation and complex structures. Lack of specific equipment, for instance, CGPS is a huge obstacle. Therefore, InSAR is a useful tool to investigate the areas where they are very difficult to access. Moreover, InSAR can preliminary assess information of the study area. With many strong advantages, InSAR is brought to displacement investigation of the study area.

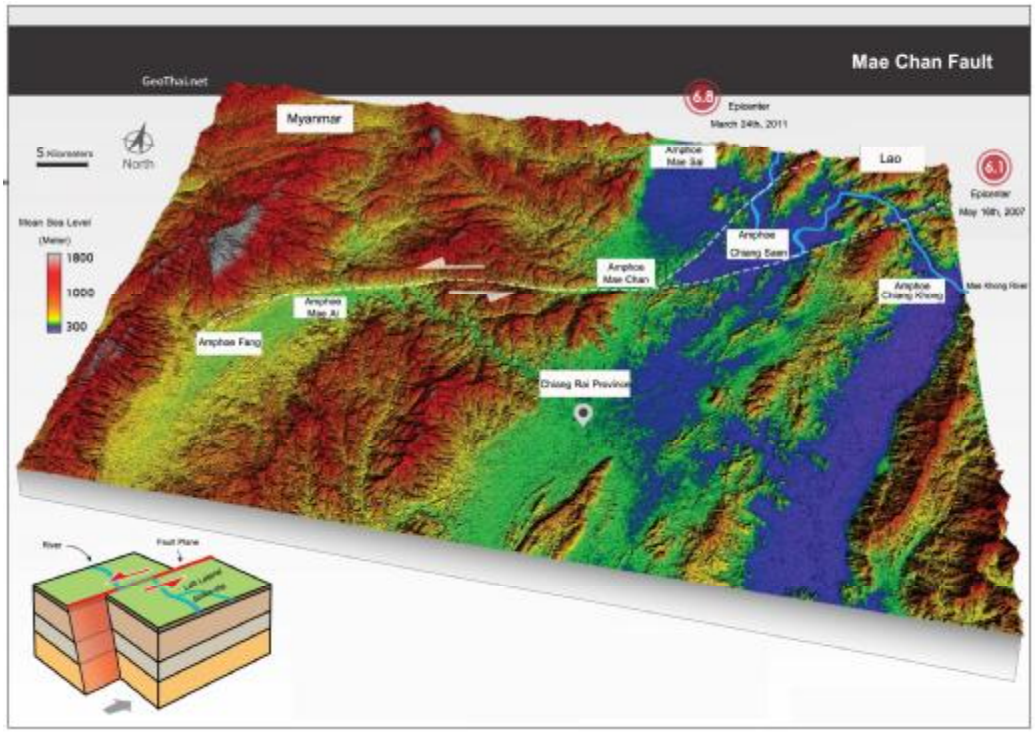

Figure 1: Location map of Mae Chan fault (Taken from a figure in http://geothai.net/gneiss/?p=204).

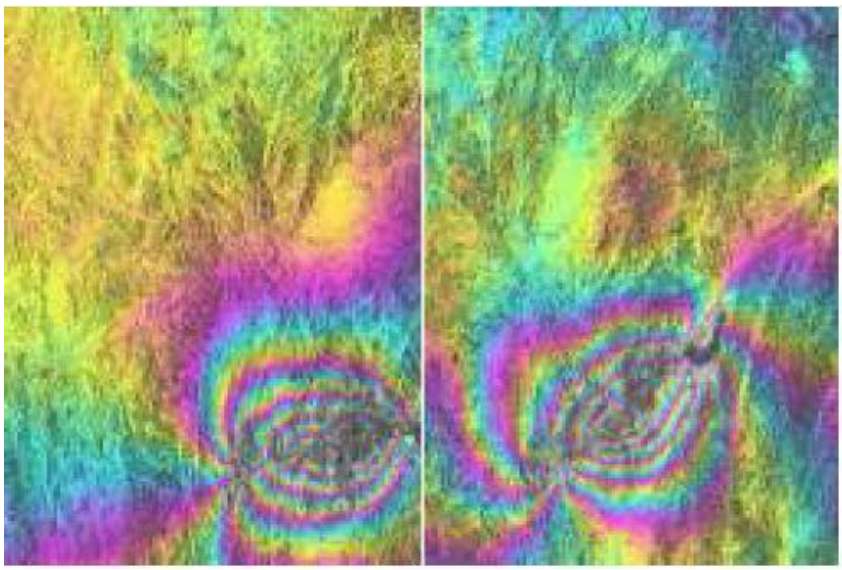

Figure 2: Unwrapped interferogram from ascending (left) and descending SAR image pair (Trisirisatayawong et al., 2011).

SAR DATA

The 27 Radarsat-2 both ascending and descending orbits imageries from June, 2011 to May, 2012 covering the Mae Chan fault area and Nam ma fault in Myanmar were brought into the process as shown in table 1. All interferograms are relative to the master image of 15 December, 2011 (Beam type: F3N, Incidence angle: 42º) and 19 November, 2011 (Beam type: F21F, Incidence angle: 36º) respectively.

Table 1: Acquisition details of Radarsat-2.

No.	Date	Beam Type	Orbit Sense	Baseline (meter)
1	30-June-2011	F3N	Ascending	-271
2	24-July-2011	F3N	Ascending	-240
3	17-August-2011	F3N	Ascending	-183
4	04-October-2011	F3N	Ascending	-173
5	28-October-2011	F3N	Ascending	172
6	21-Novevember-2011	F3N	Ascending	-98
7	15-December-2011	F3N	Ascending	0
8	08-January-2012	F3N	Ascending	-1122
9	01-February-2012	F3N	Ascending	-270
10	25-February-2012	F3N	Ascending	-341
11	20-March-2012	F3N	Ascending	-139
12	13-April-2012	F3N	Ascending	69
13	07-May-2012	F3N	Ascending	-679
14	31-May-2012	F3N	Ascending	240

No.	Date	Beam Type	Orbit Sense	Baseline (meter)
1	04-June-2011	F21F	Descending	-271
2	22-July-2011	F21F	Descending	-240
3	15-August-2011	F21F	Descending	-183
4	08-September-2011	F21F	Descending	-173
5	02-October-2011	F21F	Descending	172
6	26-October-2011	F21F	Descending	-98
7	19-November-2011	F21F	Descending	0
8	13-December-2011	F21F	Descending	-1122
9	06-January-2012	F21F	Descending	-270
10	30-January-2012	F21F	Descending	-341
11	23-February-2012	F21F	Descending	-139
12	18-March-2012	F21F	Descending	69
13	11-April-2012	F21F	Descending	-679

Figure 3: Location map of left-lateral fault system in the Golden Triangle area and footprint of Radarsat-2 SAR imagery both in ascending and descending orbits.

DATA PROCESSING USING TIME-SERIES INSAR TECHNIQUES

In this study, StaMPS/MTI software which associated with time-series InSAR technique was applied to analyze time-series data from Radarsat-2. The initial part of the processing step has been done for interferograms generation using DORIS software. This part, the 3 arc-second (90 meter) resolution of SRTM DEM was used to remove topographic phase. Pairs of Interferograms were then simultaneously processed using only phase stability in each pixel in an iterative process way. Then, phase stability which is contained in each pixel was initially rejected based on their amplitude characteristics. The Persistent Scattered (PS) selection procedure diagram is shown in figure 4 (Hooper et al., 2007).

According to figure 4, a first procedure of PS selection is to convert all data into a preferred format for PS processing. Next, phase noise which is existed in each candidate pixel of every interferogram was estimated and selected base on their noise characteristics. After that, the pixels selected in the previous step are weeded and corrected for spatially-uncorrelated look angle error (SULA) and master atmosphere and orbit error (AOE). Values of Spatially-Correlated Look Angle Error (SCLA) which is occurring from DEM and AOE were calculated and eliminated using measure of the phase noise level equation (1) as shown below (Hooper et al., 2007).

$$\gamma_x = \frac{1}{N}\left|\sum_{i=1}^{N} \exp\{i(\Delta\phi_i - \beta_i \Delta h)\}\right| \quad (1)$$

When N = Number of interferogram

$\Delta\phi_i$ = Phase differential in each Pixel

β_i = Baseline

Δh = Height differential

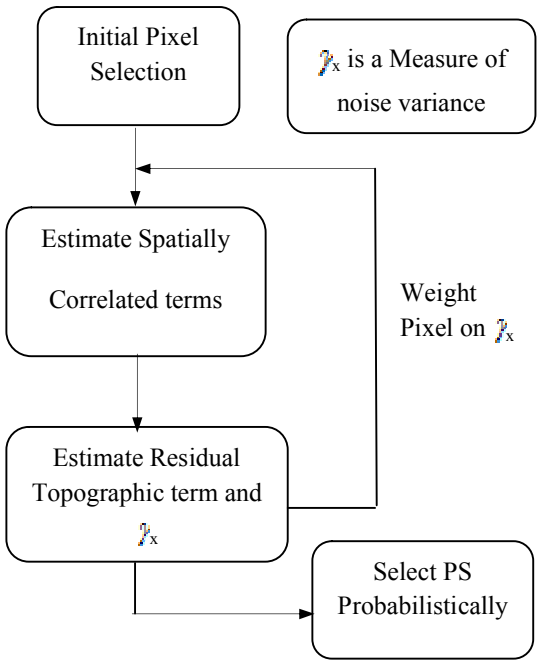

Figure 4: PS selection Algorithm (Hooper, 2009).

From equation (1), an acquired result can be calculated into radar line-of-sight direction. After finished this procedure, Persistent Scattered (PS) will be displayed as position of point detected with the deformations value of measurement.

PHASE OF THE EARTHQUAKE CYCLE

Earthquake could be described as a result of a sudden release of energy in the earth's crust that creates seismic waves. Due to information of Nam ma fault and Mae Chan fault which are left lateral fault trending, the moving trend of these faults are shown in figure 5 where earthquake cycle are explained.

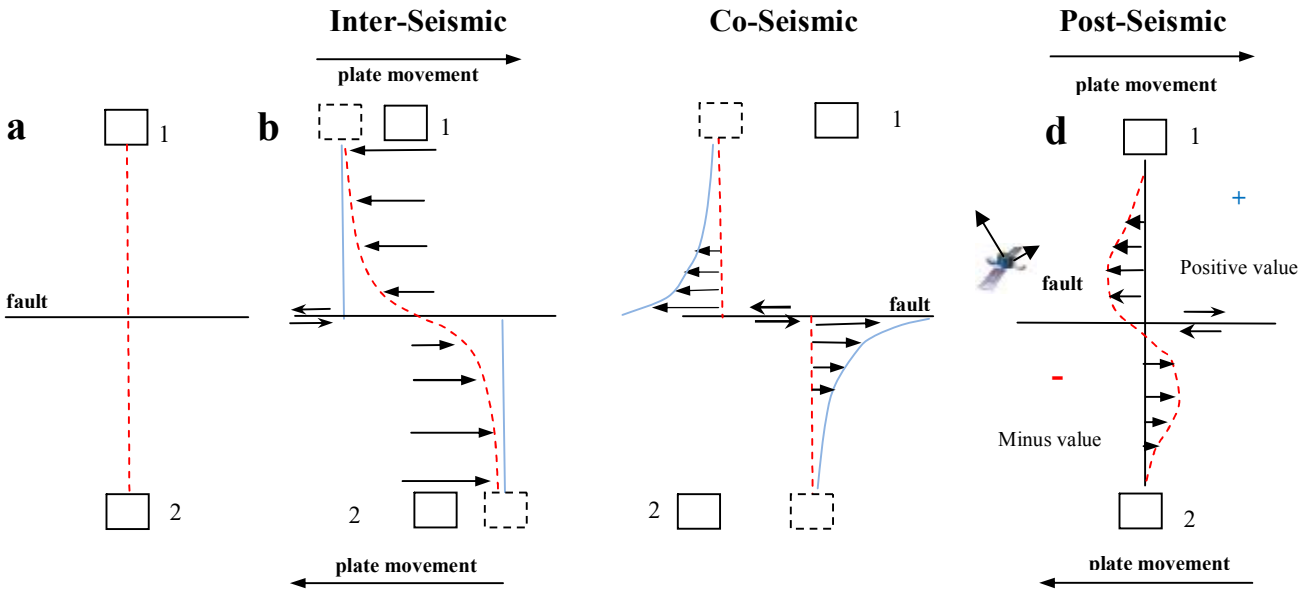

Figure 5: Earthquake cycle as explained by elastic model (modified from Wright, 2002).

Figure 5a reveals a fault plane which is located between two crusts (red-dashed line in a figure). Figure 5b shows in the red-dashed has become curved as this is known as inter-seismic motion. It reveals a procedure of strain accumulation in the earth's crust in an opposite direction. Figure 5c shows a procedure of co-seismic motion when the stress accumulation reaches a breaking point (the shear stress lager than frictional forces). The energy will be abruptly released and the earthquake is occurred. The earth's crusts are then slipped in the opposite direction. Co-seismic movements depend on the amount of fault slip and depth to which it extends (Thatcher, 1993). The blue lines in figure 5 indicate the sum of deformation before and after earthquake. After a co-seismic motion completed, the stress will be decayed this procedure called post-seismic motion. The cycle then begin again. The earth's crusts which slipped in new position still accumulated the stress and will be displayed as post-seismic deformation occurring in aftermath of an earthquake. The figure 5d was supposed that the direction of satellite in ascending orbit movement is forwarding to radar platform, so displacement rates is indicated as a positive value while the contrary is indicated as a minus value. In this procedure, SAR imageries would be brought into an analyzing process to detect a displacement in the study area.

RESULT AND CONCLUSION

The initial result which is analyzed by time-series InSAR technique reveals the post-seismic interferometric deformation of Tarlay earthquake spanning approximately one year. There are more than 147,000 PS points of ascending path with LOS displacement rate between -60.6 to 63.8 millimeters per year as shown in figure 6 while there are approximately 232,700 points of descending path with LOS displacement rate between -219.3 to 86.4 millimeters per year as shown in figure 7.

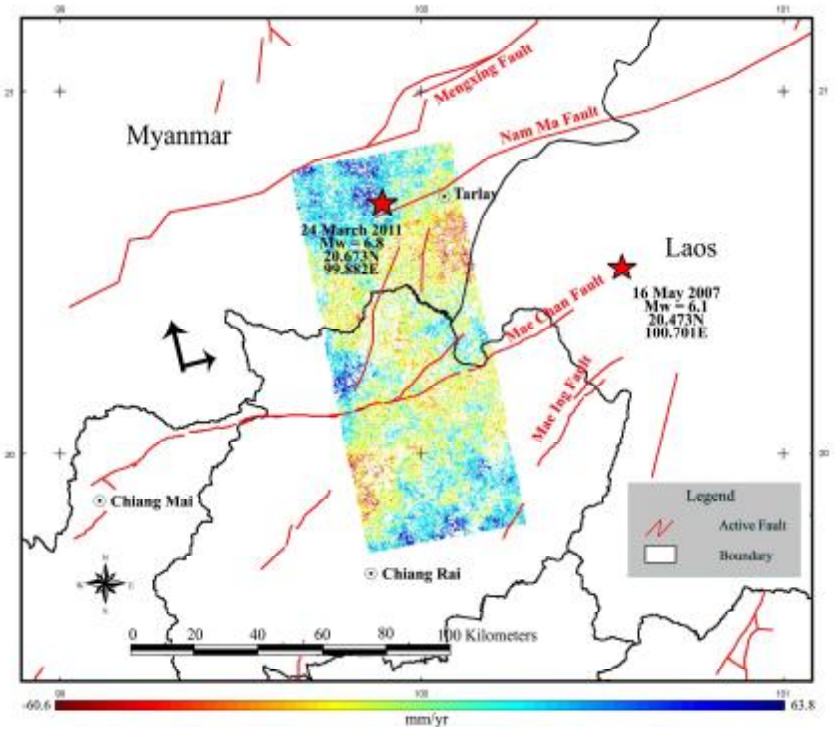

Figure 6: Post-seismic LOS displacement rate (mm/year) in Mae Chan and Nam Ma faults from Radarsat-2 imagery beam type: F3N ascending path using time-series InSAR method.

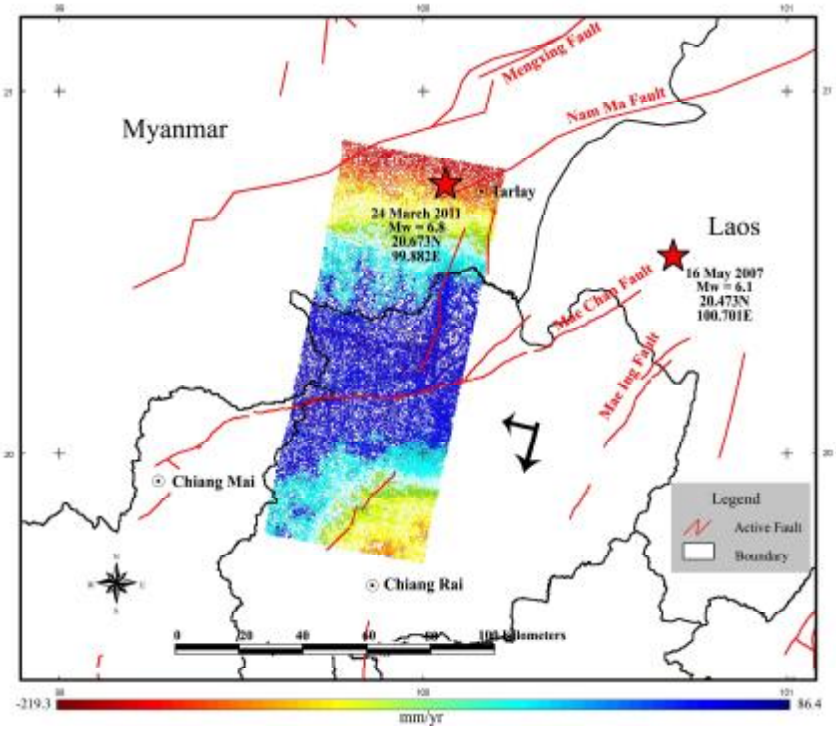

Figure 7: Post-seismic LOS displacement rate (mm/year) in Mae Chan and Nam Ma faults from Radarsat-2 imagery beam type: F21F descending path using time-series InSAR method.

The mean velocities are calculated in radar line-of-sight direction. The results indicated a procedure of stress accumulation in this area could be probability of earthquake in the future and provided detail on how crust movements continued after co-seismic previous studies. Although the whole pattern of PS point is complicated due to decorrelation and atmosphere errors, but remarkable surface deformation can still be observed. Hanssen (2005), presented standard deviation of estimated deformation and topography graph in his research and the result revealed that the precision standard deviation of velocity and topography improve with increasing number of acquisitions. Thus, to improve accurate post-seismic deformation, more Radarat-2 imageries are required for reducing the causes of inaccuracies from the technique.

ACKNOWLEDGEMENT

The authors thank the Geo-Image Technology Research Unit, Department of Survey Engineering, and Chulalongkorn University for facilities support. The Radarsat-2 SAR data used in this work are provided by Geo-Informatics and Space Technology Development Agency (GISTDA) cooperating with Canadian Space Agency (CSA) and MacDonald, Dettwiler and Associates Ltd. (MDA). Finally, we would like to thank Mineral Resources Department's Active Fault Research Division for their support in active fault data.

REFERENCES:

Hanssen, R.F., 2005. Satellite radar interferometry for deformation monitoring: A priori assessment of feasibility and accuracy. International Journal of Applied Earth Observation and Geoinformation, 6 (3-4), pp. 253-260.

Hooper, A., Segall, P. and Zebker, H., 2007. Persistent scatterer interferometric synthetic aperture radar for crustal deformation analysis, with application to Volcáno Alcedo, Galapagos. Journal of Geophysical Research, 112 (B07407), pp. 21.

Hooper, A., 2009. Satellite Radar Interferometry: Methodology, Quality Control and Application Development. In: Presentation of InSAR Workshop, 23- 27 March 2009, Chulalongkorn University, Bangkok, Thailand.

Jitmahantakul, S., 2011. Mae Chan fault. Article published (online). Available from: http://geothai.net/gneiss/?p=204 [2011,March].

Thatcher, W., 1993. The earthquake cycle and its role in the long-term deformation of continental lithosphere. Annali Di Geofisica, 36 (2), pp. 13-24.

Trisirisatayawong, I., Hooper, A., and Aobpaet, A., 2011. Co-seismic Displacement of 24-March- 2011 Mw 6.8 Mong Hpayak Earthquake, Myanmar. In: Proceeding of the FRINGE Workshop 11, 19-23 September 2011, ESA-ESRIN, Frascati (Rome), Italy.

Wright, T.J., 2002. Remote monitoring of the earthquake cycle using satellite radar interferometry. Philosophical Transactions of the Royal Society of London, 360 (1801), pp. 2873-2888.

McCaughey, J., and Tapponnier, P., 2011. Myanmar earthquake of March 24, 2011 - Magnitude 6.8. Article published (online). Available from: http://www.earthobservatory.sg/media/news-and-features/295-myanmar-earthquake-of-march-24th-magnitude-68.html) [2011,March].